Flow-based arterial spin labeling: from brain to body

Franklin, S.L.

Chapter 5

Arterial Spin Labeling using Spatio-temporal Encoding (SPEN) readout for robust perfusion imaging in inhomogenous magnetic fields

S.L. Franklin[1,2], M. Schuurmans[1], M. Otikovs[3], P. Borman[4], M.J.P. van Osch[2,5], C. Bos[1].

[1]Center for Image Sciences, University Medical Center Utrecht, Utrecht, The Netherlands
[2]C.J. Gorter Center for High Field MRI, Department of Radiology, Leiden University Medical Center, Leiden, The Netherlands.
[3]Department of Chemical and Biological Physics, Weizmann Institute of Science, Rehovot, Israel.
[4]Department of Radiotherapy, University Medical Center Utrecht, Utrecht, The Netherlands
[5]Leiden Institute for Brain and Cognition, Leiden University, Leiden, The Netherlands.

ABSTRACT

Purpose: To evaluate the feasibility of spatio-temporal encoding (SPEN) readout for pseudo-continuous ASL (pCASL) in brain, and its robustness to susceptibility artifacts as introduced by aneurysm clips.

Methods: A 2D self-refocused T_2*-compensated hybrid SPEN scheme, with super-resolution reconstruction, was implemented on a 1.5T Philips system. Q (= BW_{chirp}*T_{chirp}) was varied, and, the aneurysm clip-induced artifact was evaluated, in a phantom (label-images) and in-vivo (perfusion-weighted signal (PWS)-maps and temporal signal-to-noise (tSNR)). In-vivo results were compared to gradient-echo echo-planar-imaging (GE-EPI) and spin-echo EPI (SE-EPI). tSNR as a function of repetition time (TR) was compared between SPEN and SE-EPI. SPEN with Q~75 encodes with the same off-resonance robustness and resolution as EPI.

Results: The clip-induced artefact with SPEN decreased as a function of Q, and wassmaller than with SE-EPI and GE-EPI in-vivo. tSNR decreased with Q and the tSNR of GE-EPI and SE-EPI corresponded to SPEN with a Q-value of approximately ~85 and ~108, respectively. In addition, SPEN perfusion images showed a higher tSNR ($p<0.05$) for TR=4000 ms compared to TR=2100 ms, while SE-EPI did not. tSNR remained relatively stable when the time between SPEN-excitation and start of the next labeling-module was more than ~1000 ms.

Conclusion: Feasibility of combining SPEN with pCASL imaging was demonstrated, enabling cerebral perfusion measurements with a higher robustness to field inhomogeneity (Q>75),at no cost to tSNR and resolution compared to SE-EPI and GE-EPI. Future developments are needed to enable 3D scanning and increase acquisition speed to allow smaller voxel sizes in combination with larger FOVs.

INTRODUCTION

Arterial Spin Labeling (ASL) is a non-contrast enhanced perfusion method, used for numerous applications both in brain[13], [147] as well as body[19], [62], [125], [148]–[150]. ASL is often used in combination with single-shot acquisition techniques, such as echo-planar imaging (EPI), because of their time efficiency, and motion insensitivity, which is especially important for body applications[19], [62]. However, EPI is especially prone to distortion and chemical shift artifacts in the phase-encoding (PE) direction, due to weak gradients. Many body applications, such as imaging of kidney[62], breast[151], but also brain applications, e.g. in patients with implants[152] or cerebral hemorrhages[153], [154], are characterized by magnetic field distortions, complicating the application of ASL.

Spatio-temporal encoding (SPEN) has been introduced in 2005[155] as an alternative to EPI and can provide increased robustness to magnetic field inhomogeneity in similar acquisition time[63]. In functional[156] as well as diffusion-weighted[157] MRI, SPEN was shown to be superior to EPI in areas associated with susceptibility-effects, such as the (orbito)frontal cortex of the brain[156], [158], breast[157] and in the vicinity of metal implants[159], [160].

SPEN uses a frequency-swept (chirp) pulse in combination with a gradient, which leads to a local excitation, that excites the field-of-view (FOV) over time. This results in a linear relationship between spatial location and time, and thus no Fourier transformation is required in the direction of this excitation gradient. Super-resolution (SR) reconstruction is performed to enable short scan times without compromising on resolution or SAR, compared to EPI[161], [162]. SPEN is characterized by a stronger mean acquisition gradient (G_{acq}) as compared to EPI (Figure 1), which reduces image distortion (displacement (d)) as a result of susceptibility-effects: $d = \frac{\Delta B_0}{G_{acq}}$. Sensitivity to susceptibility-effects can further be reduced by full T_2*-refocusing of all data, when using appropriate timings. However, the frequency swept pulse in SPEN could potentially saturate incoming blood (i.e. blood below the labeling plane), which would in turn reduce labeling efficiency during the following labeling module, thereby necessitating a longer repetition time (TR) to preserve temporal SNR (tSNR).

In this technical note, the feasibility of combining SPEN with pseudo-continuous ASL (pCASL) for cerebral perfusion imaging was explored: 1) The behavior of SPEN as a function of Q (= BW_{chirp}*T_{chirp} [-]), which determines the robustness to susceptibility-effects and SNR, is investigated in the presence of an aneurysm clip, in a phantom, and 2) in-vivo. 3) The perfusion-weighted signal (PWS)-map, in the presence of an aneurysm clip, is compared between SPEN,gradient-echo (GE-)EPI and spin-echo (SE-)EPI. 4) The effect of TR on the temporal signal-to-noise (tSNR) of the PWS-images for SPEN and SE-EPI is investigated.
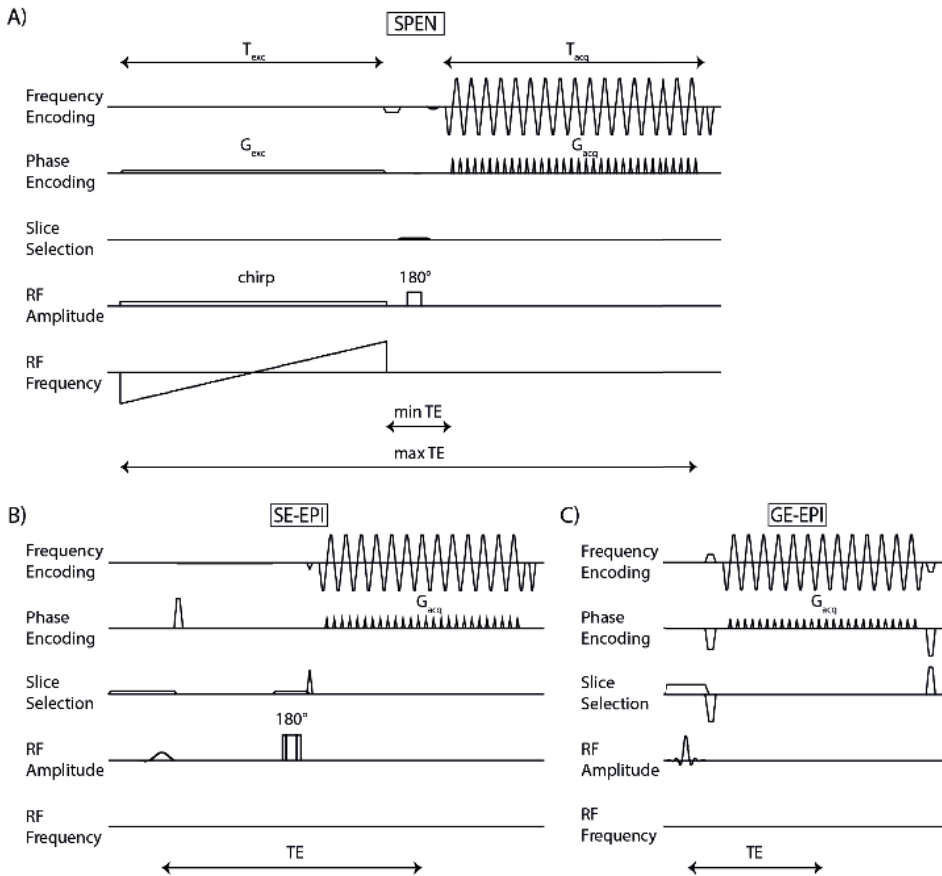
Figure 1. Scaled sequence diagrams for the A) SPEN (Q=125), B) SE-EPI, and C) GE-EPI readout, used in this study. The acquisition gradient (G_{acq}) in phase-encoding direction, is larger for SPEN compared to GE-EPI and SE-EPI, leading to a larger robustness for magnetic field offsets. For SPEN, the frequency-swept chirp-pulse is used as excitation pulse. The chirp-pulse in combination with the 180-degree refocusing pulse, results in sequentially generated echoes in time, related to different parts of the field-of-view. This leads to a varying T_2-weighting over the field-of-view: spins that are first excited will have a maximum TE, while spins that are excited last will have felt a minimum TE. The excitation time (T_{exc}) was chosen equal to the acquisition time (T_{acq}), resulting in full-T_2* refocusing.

METHODS

Data acquisition

This study was approved by the local ethics committee (METC Utrecht, Protocol 15-466) Informed consent was obtained from all participants. Nine healthy volunteers (six females, 26-32 years), were scanned on an 1.5T Philips Achieva scanner (Philips, Best, The Netherlands) using an 8-channel head coil.

A 2D self-refocused T_2*-compensated hybrid SPEN scheme was used, where SPEN encoding in the original PE direction, i.e. anterior-posterior, was combined with conventional k-space

encoding in the frequency-direction[63]. The sequence included; a 90-degree chirp-pulse with a duration equal to the acquisition duration ($T_{chirp} = T_{acq} = 20.4$ ms); and a 180-degree spin-echo pulse, positioned symmetrically in between the chirp-pulse and start of acquisition, to ensure complete T_2^*-refocusing (Figure 1). Depending on Q, B_1, G_{exc} and G_{acq} were adjusted according to: $B_1 = 0.27 * \frac{\sqrt{Q}}{\gamma T_{exc}}$ [163], $G_{exc} = \frac{Q}{\gamma L_{pe} T_{exc}}$, and $G_{acq} = \frac{Q}{\gamma L_{pe} T_{acq}}$ (L_{pe} = field-of-view in SPEN-direction). SPEN was acquired with a field-of-view (FOV) of 200 x 200 mm, slice thickness of 10 mm, voxel size of 3.1 mm in read-direction, and Δy_{spen}=5.7 mm in SPEN-direction, which is defined by the shift of the quadratic phase-profile between readout lines. This results in a TE range of 5-45 ms over the FOV. All scans were acquired with slope sampling turned off, and all in-vivo scans were acquired with Spectral Presaturation with Inversion Recovery (SPIR) fat suppression.

For all in-vivo scans, separate M_0-images were acquired with the same readout and Q-value setting, by turning ASL labeling off and TR=2000 ms, resulting in durations of 8 s.

Experiment 1:
A phantom and aneurysm clip (titanium, 2 cm), see Supporting Information Figure 1, were placed in water doped with 0.4 mM Gd. SPEN was acquired with Q-values of; 50, 75, 100, 12, 150 and 200, each corresponding to an off-resonance robustness (BW/mm) of 12.3 Hz/mm, 18.3 Hz/mm, 24.7 Hz/mm, 30.7 Hz/mm, 36.6 Hz/mm and 49.4 Hz/mm. This series was acquired with and without SPIR.

Experiment 2:
Two healthy volunteers were scanned with the aneurysm clip, positioned on the forehead and fixated by tape. ISPEN was acquired with Q-values; 50, 75, 100, 125, and 150. In volunteer 2, an image with Q = 175 was additionally acquired, corresponding to 43.0 Hz/mm.

SE-EPI and GE-EPI-scans were acquired with the same FOV and slice thickness, acquired voxel size of 3.1 mm x 3.0 mm, SENSE factor of 1.3, and TR of 4000 ms. The TE was 17 ms, and 9.1 ms, for SE-EPI and GE-EPI, respectively. These settings correspond to a BW/mm of 18.7 Hz/mm. So, the off-resonance robustness, and thus PE/SPEN bandwidth, of SE-/GE-EPI is similar to SPEN with Q~75. Meaning that the resolution of SPEN with Q≥75 after SR-reconstruction is as least as high as EPI[164].

These scans were acquired with pCASL labeling duration of 1800 ms, background suppression, and post-label delay (PLD) of 1800 ms and 30 repetitions. Background suppression included presaturation of the imaging stack just before start of labeling, and two non-selective hyperbolic secant pulses at 2250ms and 3150ms after presaturation. The total scan duration was 4 min 16 s for SPEN and SE-EPI, and 4 min 8 s for GE-EPI-scans.

In addition, in volunteer 2, a T_1-weighted scan without the aneurysm clip was acquired, using multi-slice single-shot SE-EPI, FOV of 230 x 183mm, voxel sizes of 0.9 x 1.12 x 5 mm, 21 slices, and TR/TE of 570 ms/15 ms.

Experiment 3:

In the same volunteers of experiment 1, additional pCASL-scans with SPEN, SE-EPI and GE-EPI readout were acquired without an aneurysm clip positioned on the forehead, using the same settings.SPEN was acquired with Q=125 and Q=175for volunteer 1 and 2, respectively.

Experiment 4:

Six volunteers were scanned with a series of SPEN and SE-EPI-scans, where TR was varied according to: 2100 ms, 2300 ms, 2600 ms, 3000 ms, 3500 ms, and 4000 ms. SPEN-scans were acquired with Q=50 (12.4 Hz/mm). For the SE-EPI scans, the same settings were used as described in experiment 2. Scans were acquired with a labeling duration of 1000 ms, PLD of 1000 ms, and 30 repetitions. Scan durations were the same for SPEN and SE-EPI, ranging between 2 min 14 s and 4 min 16 s for TRs of 2100 ms and 4000 ms, respectively. Background suppression was turned off. In addition, a T_1-weighted scan was acquired.

Data analysis

K-space data of the SPEN-images were exported from the scanner, and pre-processing, up to (not including) the Fourier-transformation, of the data was done using ReconFrame (Gyrotools, Zurich, Switzerland). The data was reconstructed following steps described by Seginer et al[165], by adapting the algorithm[166], where instead of L2-regularized iterative reconstruction used in reference[166], final images were obtained by a multiplication with a SR matrix[64].

Co-registration and motion correction was performed using a rigid PCA-based registration method[114] using Mevislab (MeVis Medical Solutions, Bremen, Germany). SPEN, SE-EPI and GE-EPI-scans were all separately co-registered to the T_1-scan. Perfusion-weighted maps were calculated using:

$$\Delta S_i = \frac{1}{R} \sum_{r=1}^{R} (C_{r,i} - L_{r,i})$$

(1)

$$PWS_i[\%] = \frac{\Delta S_i}{M_{0,i}}$$

(2)

Where: $C_{r,I}$ = control-image, $L_{r,I}$= label-image, r= repetitions, i= voxels, ΔS_i= subtraction-image, $M_{0,i}$= the scan used to calibrate the ASL-signal according to the expected blood signal[13]. Brain masks, used for visualization of the PWS-maps, were generated using SPM (Wellcome

Center for Human Neuroimaging, London, United Kingdom), based on the M_0-scans acquired without aneurysm clip. GM segmentation was performed on the T_1-weighted scans using SPM(using >70% GM contribution)

tSNR maps were generated using:

$$\text{tSNR}_i = \frac{\mu_{\Delta S,i}}{\sigma_{\Delta S,i}} \tag{3}$$

Where $\mu_{\Delta S,i}$= mean ASL-signal over all repetitions, and $\sigma_{\Delta S,i}$= standard deviation over time. The tSNR in GM was calculated by averaging the tSNR in all GM voxels.

Experiment 1
Label-images were generated for each Q-value.

Experiment 2
Label-images, M_0-images, PWS-maps, and tSNR-maps were generated for each Q-value. To calculate mean tSNR in GM, the part of the FOV containing the clip-induced artifact was omitted from the GM-mask, by taking out a square of 1/3 of FOV. To compare the tSNR in GM of SPEN, GE-EPI and SE-EPI, the tSNR of the EPI-images was corrected by a factor $\Delta y_{SPEN}/\Delta y_{EPI}$ to compensate for the smaller voxel sizes, with Δy_{EPI} the acquired voxel size of the EPI-scans.

Experiment 3
Label-images and PWS-maps were generated for SPEN, SE-EPI and GE-EPI with and without aneurysm clip.

Experiment 4
tSNR maps, and the average tSNR in GM over all volunteers was calculated for each TR, for SPEN and SE-EPI. A non-parametric Wilcoxon rank sum test (α=0.05), was used to test whether the tSNR of TR=2100 ms was significantly different from TR=4000 ms.

RESULTS

A higher Q-value decreases the aneurysm clip-induced artefact, as demonstrated in a phantom, see Figure 2A. This effect reduces when using SPIR, see Figure 2B. In both cases, additional through-plane slice-selection effects lead to signal voids near the aneurysm clip, see Supporting Information Figure 1. In-vivo, SPIR was deemed necessary, and thus the effect of Q on the clip-induced artefact size is reduced, see Supportng Information Figure 2.
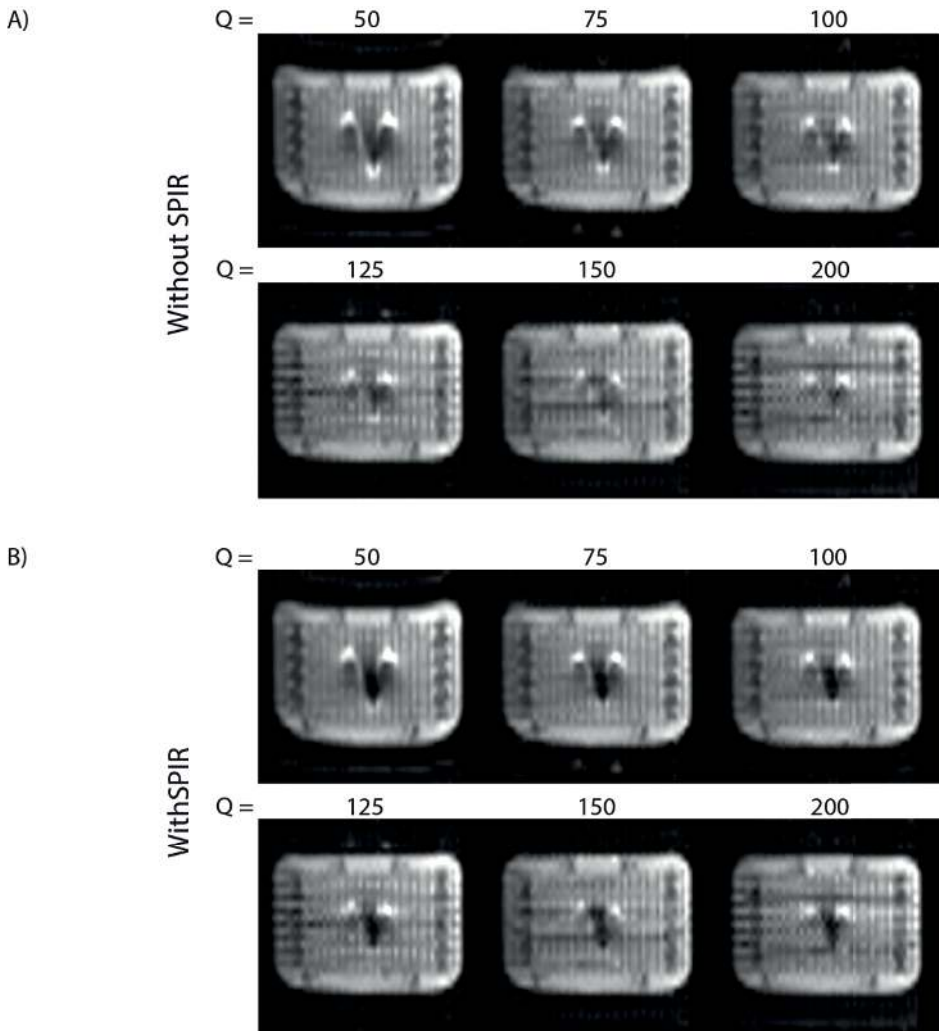
Figure 2. Phantom with aneurysm clip, acquired with a SPEN-readout at different Q-values (50,75,100,125,150,200), A) without SPIR fat suppression, B) with SPIR fat suppression. The artefact induced by the aneurysm clip is reduced for higher Q-values (A). This effect becomes less apparent when using SPIR fat suppression (B). Signal intensity is normalized per Q-value to facilitate comparison of field inhomogeneity effects between the images.

The label-images show some ghost artifacts for higher Q-values (> ±125), indicated by black arrowheads in Supportng Information Figure 2A. The tSNR of the PWS-images shows a $1/\sqrt{Q}$-relation, and the tSNR of SE-/GE-EPI correspond to the tSNR of SPEN with Q=108/85 respectively, see Figure 3.

The aneurysm clip-induced artifact is smaller for the SPEN compared to SE-/GE-EPI, and SE-EPI and GE-EPI show additional artifacts, see Figure 5. In the PWS-maps, small subtraction

artifacts can be observed at the location of the aneurysm clip for SE-EPI and GE-EPI, which are not visible for SPEN, see Figure 4.
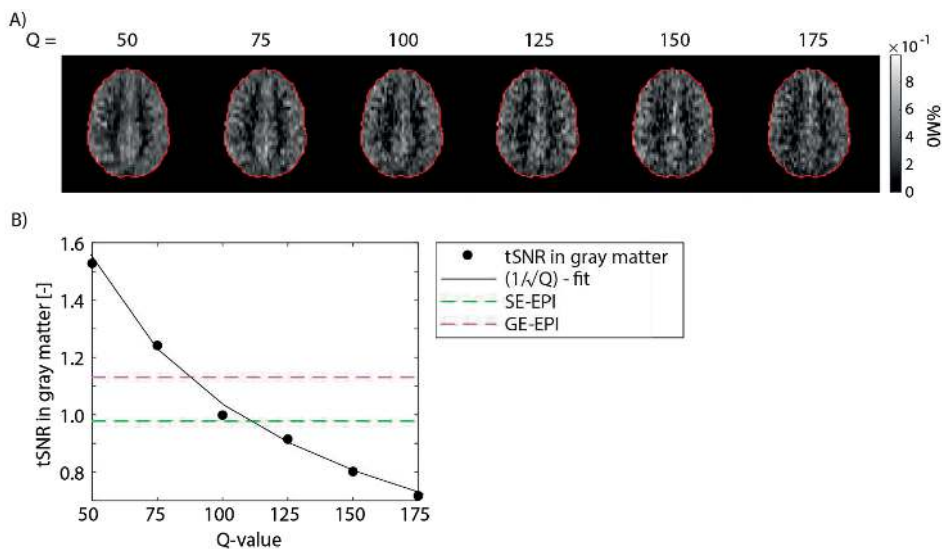

Figure 3. A) SPEN perfusion-weighted signal (PWS)-images at Q-values between 50-175. B) Mean temporal SNR (tSNR) in gray matter as a function of Q-value. The data is fitted with a 1/√Q – function. The tSNR-value of SE-EPI and GE-EPI, corrected for acquisition voxel size, are illustrated with a dotted line in green and magenta, respectively.
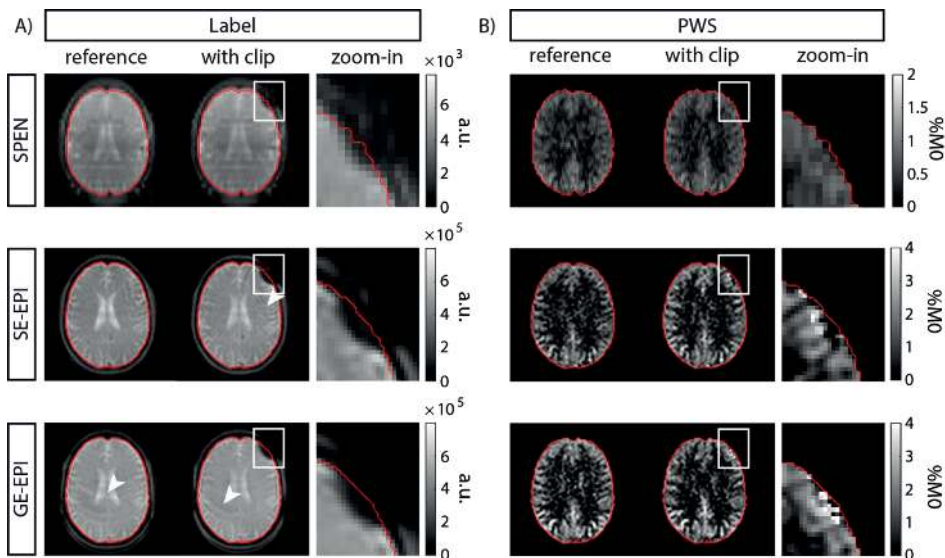

Figure 4. Comparing the effect of an aneurysm clip on SPEN with Q = 125, SE-EPI and GE-EPI. A) pCASL label images, and B) perfusion-weighted signal (PWS) maps, without (reference) and with (with clip) aneurysm clip. The last column shows a zoom-in of the artifact area, of which the exact location is depicted by the white square. The clip-induced artifact is smaller for SPEN compared to SE-EPI and GE-EPI. In addition, SE-EPI showed a Gibbs ringing artifact anterior to the aneurysm clip, and GE-EPI showed ghost artifacts, both indicated by white arrows.

tSNR increases noticeably with TR for SPEN, see Figure 5A. This trend was confirmed by quantitative evaluation of tSNR over all volunteers, see Figure 5B. tSNR was significantly different between the TR=2100 ms and TR=4000 ms for SPEN (p = 0.026, median difference = 0.551), and not for SE-EPI (p = 0.240, median difference = 0.207).
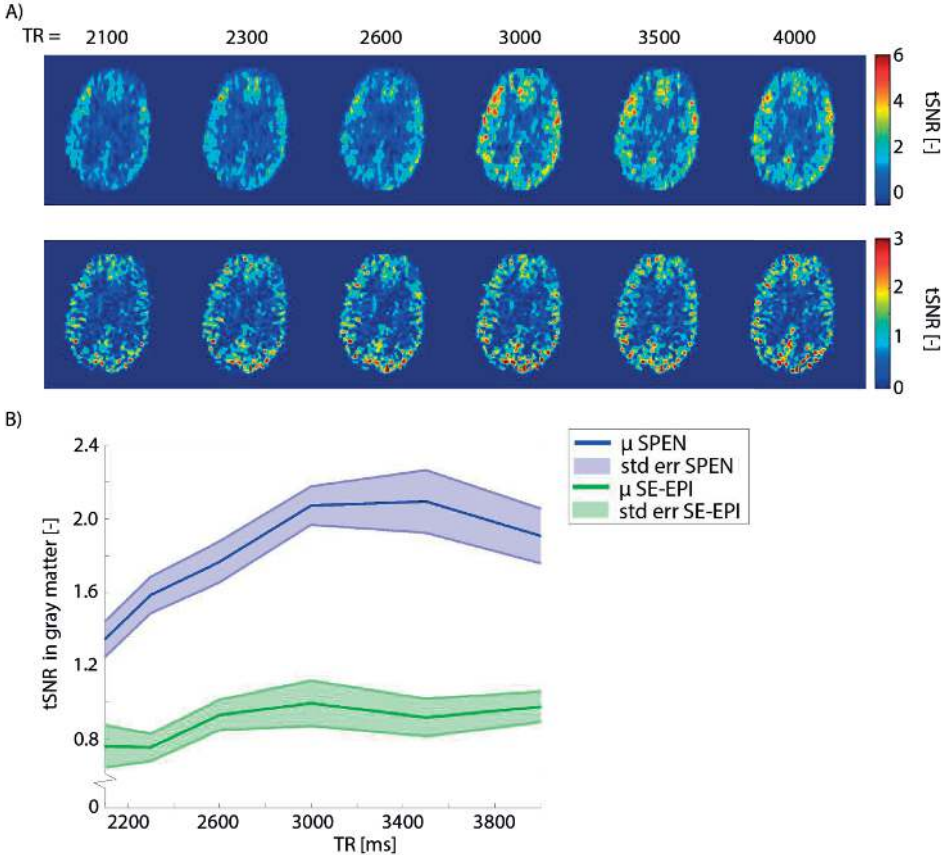

Figure 5. A) Effect of TR on SPEN and SE-EPI for a representative volunteer. B) Mean (μ) normalized tSNR in gray matter over all volunteers as a function of TR, for SPEN (blue) and SE-EPI (green). tSNR was normalized with respect to the value at a TR of 4000 ms. The shaded area represents the standard error (st. err.) of tSNR.

DISCUSSION

Results showed the feasibility of SPEN in pCASL imaging, enabling cerebral perfusion measurements with a higher robustness to susceptibility-effects compared to SE-/GE-EPIPI, at no cost to tSNR or resolution, by using the appropriate Q-value. The $1/\sqrt{Q}$-relation between tSNR of SPEN and Q-value, as previously derived in reference[162], was confirmed. Furthermore, a dependence on TR was observed for pCASL-images acquired with SPEN.

meaning that every acquired point was close to being completely refocused (instead of just the center of k-space), reducing signal loss due to T_2^*[63]. Experiment 1 and 2 showed that SPEN had a smaller clip-induced artifact than SE-EPI and GE-EPI, for all Q-values, confirming the higher robustness to field-inhomogeneity of SPEN. Similar as was observed in the vicinity of metallic implants[160]. Increasing Q results in stronger acquisition gradients[64], so smaller distortions as a result of field inhomogeneities are expected. Results showed a reduction in the clip-induced artefact for higher Q-values, evidencing a higher robustness to susceptibility-effects. In-vivo, the clip-induced artifact remained relatively stable over Q. This is likely mainly due to the suppression of water signal, caused by sensitivity to off-resonance of SPIR, as well as through-plane effects caused by distorted excitation profiles[167] due to limited bandwidth of the slice-selective refocusing pulse, both demonstrated in the phantom data. SPEN enables robust imaging via two mechanisms: SPEN has a stronger G_{acq} resulting in reduced image distortions as a result of susceptibility-effects[63].Secondly, SPEN was acquired in full-refocusing mode,

tSNR in GM of SPEN dropped according to $1/\sqrt{Q}$, confirming the theoretical derivation by Ben-Eliezer et al[162]. With Q the quadratic phase-profile narrows, resulting in a lower SNR. Using the current settings, the GM tSNR of SE-EPI and GE-EPI corresponded to SPEN with a Q-value of approximately ~85 and ~108, respectively, based on the $1/\sqrt{Q}$-curve. Importantly, the G_{acq} of SPEN is higher than of SE-/GE-EPI, at Q=85 and 108, since the BW/mm of SE-EPI and GE-EPI corresponds to Q~75. Meaning that if Q≥75 and Q≤108(SE-EPI) or Q85≤(GE-EPI)) SPEN can produce perfusion images with higher robustness to field homogeneities, at no cost to tSNR and resolution.

For Q≥±125, ghost artifacts were observed. They are a result of the SR reconstruction and are akin to Nyquist ghosts seen in EPI-readouts[165]. These artifacts can be prevented by acquiring more points in the SPEN-direction or by using alternative post-processing techniques[168]. However, the former would inevitably increase ASL-signal loss due to T_2-decay. The longest TE in SPEN is equal to $T_{exc} + T_{acq} + TE_{min}$ (time in between the chirp-pulse and the start of acquisition, see Figure 1). So the requirement to limit TE results in constraints on the maximum achievable FOV and acquisition matrix. Multi-shot 2D SPEN[160] could be an alternative, but in line with most common body ASL protocols[169], we opted to stick to a single-shot readout. In contrast to SPEN, voxel sizes of SE-/GE-EPI could be chosen smaller without a large penalty on TE, partly due to the use of parallel imaging. Recent developments exploring parallel imaging methods for SPEN have been introduced, e.g. by simultaneously acquiring separate parts of the FOV using multi-band chirp pulses[157], [161], [170] or by acquiring low-resolution images and employing k-space interpolations, based on multiple-receivers, to increase resolution[164].

Experiment 3 furthermore demonstrated that, when using a short pCASL labeling duration and PLD to become sensitive to the start of the bolus, a higher tSNR for SPEN is observed at longer TRs, which was not the case for SE-EPI. Background suppression was turned off to prevent additional effects on the signal-evolution. The tSNR of SPEN followed a recovery-like pattern over TR, approaching an equilibrium for long TR (> 3000 ms). The results are in accordance with the hypothesis that the chirp-pulse of the previous SPEN readout saturates incoming blood, anterior to the labeling slab, thereby reducing pCASL labeling efficiency. Increasing the TR, and thus the time between end of the SPEN-readout and start of labeling, allows the inflow of fresh blood, removing this effect. From a TR of approximately 3000 ms, i.e. a pause of 920 ms, this effect was negligible, showing that sufficient fresh inflow, together with relaxation, can mitigate the saturation effects.

LIMITATIONS

All scans were performed at 1.5T, even though most ASL is performed at 3T. As ASL is increasingly being used for body applications, studies will more frequently be done at 1.5T. The advantages of smaller B_0- and physiological artefacts might outweigh the SNR-loss and shorter T_1 of blood. In addition, when scanning patients with implants the lower field strength might be advantageous. Still, it would be interesting to investigate the performance of SPEN at 3T in future studies.

A single-slice 2D SPEN sequence was used. The use of a frequency swept pulse is inherently challenging to combine with multi-slice imaging. Various approaches for multi-slice and 3D imaging have been published, while SAR and SNR limitations are considered [161], [171]–[173], providing an interesting future direction to enable whole-brain ASL with SPEN in an acceptable scan time.

In the comparison between SPEN, and SE-/GE-EPI, a relatively high Q-value (=125) was used for SPEN, meaning that the encoded resolution was higher for the SPEN than the EPI-readouts. This inevitably resulted in lower PWS-values for SPEN. Importantly, it is possible to acquire SPEN without a penalty onresolution and tSNR while preserving the smaller clip-induced artifact.

Next to EPI, other readouts are used for ASL. In brain, 3D segmented methods, such as relaxation enhancement (RARE) stack of spirals or GRASE are recommended[13], which are more robust to field inhomogeneity than EPI[174], [175]. Also in body ASL, RARE with various approaches to shorten acquisition time[176], [177] and single-shot 3D GRASE have been introduced[18]. Phase-encoded xSPEN has previously been shown to have similar resolution

and SNR as RARE, but in half the scan time[178]. Future studies making a direct comparison between SPEN and RARE approaches are necessary. The current study focused on brain measurements in the presence of an implant, as a first attempt for SPEN-ASL. For future studies, it would be interesting to combine SPEN with ASL in body applications.

Conclusion

The study showed the feasibility of SPEN-ASL and demonstrated the performance in the vicinity of an aneurysm clip implant. In addition, considerations have been raised concerning a minimal pause of ~1000 ms between the SPEN-excitation pulse and the start of the next labeling module. ASL-images acquired with SPEN benefit from a higher robustness to field inhomogeneity. By choosing an appropriate Q-value, there is no cost to tSNR or resolution, when comparing it to SE-EPI and GE-EPI. However, developments need to be made to increase acquisition speed, to allow smaller voxel sizes in combination with larger FOVs, and enable 3D-scanning.

ACKNOWLEDGEMENTS

SUPPORTING INFORMATION FIGURES
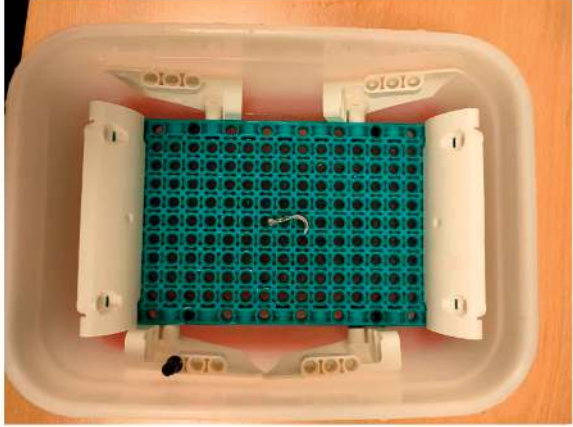
Supporting Information Figure 1. A) Titanium aneurysm clip (2 cm), used in the phantom and in-vivo scans, placed on the phantom; a plastic grid with 8.0 mm periodicity. B) Reformat demonstrating the distortion of the slice profile, indicated by white arrowheads, of the phantom as shown in A). Images were to demonstrate the through-plane effect.
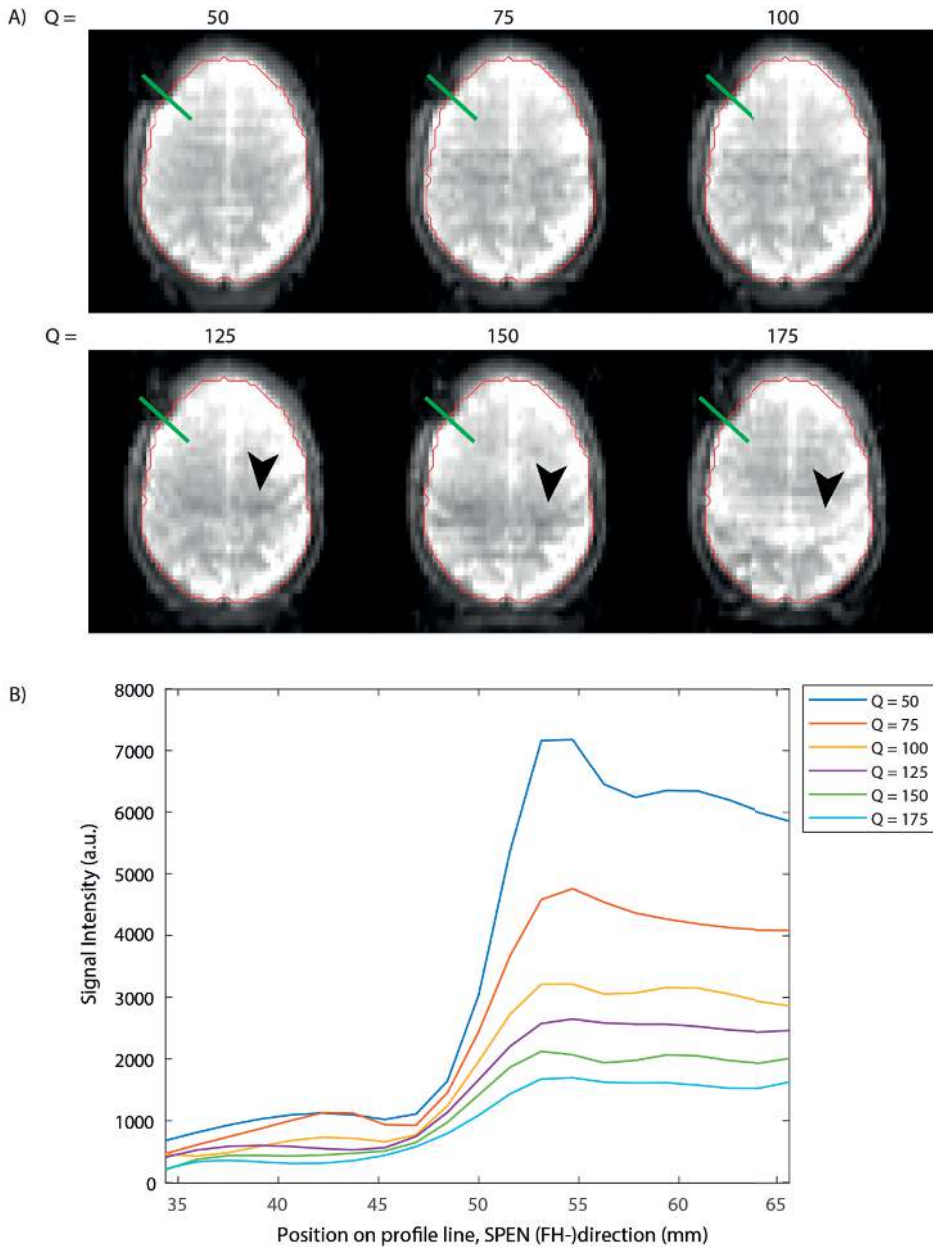
Supporting Information Figure 2. SPEN label-images for Q-values ranging between 50 and 175. A) SPEN Label images, edge artifacts are visible for higher Q-values as a result of too few measurement points, indicated by black arrowheads B) Intensity profiles along the green line in A, for all Q-values, using a spline interpolation with a factor of 2. The intensity step remains roughly at the same location for the different Q-values.

APPENDIX: THEORETICAL BACKGROUND OF SPATIO-TEMPORAL ENCODING

Single-shot echo planar imaging (EPI) is an often used readout method in ASL. It is mainly used because of its time efficiency and motion insensitivity, which is especially important in body imaging[19], [62]. However, the speed of EPI comes at the cost of B_0-sensitivity, especially in the phase-encoding direction. It can present itself as various artifacts: distortion; due to local changes to the Larmor frequency, chemical shift; due to shielding effects in the molecular environment of the hydrogen nuclei, and signal drop out; due to increased intra-voxel spin-dephasing which shortens the local T2'[179].

Distortion and chemical shift artifacts occur because the strength of the acquisition gradient in phase-encoding direction G_{acq} is relatively small[179]. Which means that if there is a small deviation in the main magnetic field ΔB_0, it leads to a large displacement Δd. For simplicity we will assume a constant gradient:

$$\Delta d = \frac{\Delta B_0}{G_{acq}} \tag{1}$$

The resolution in the phase-encoding direction in EPI is determined by the strength of the acquisition gradient G_{acq}. Note, here G_{acq} is defined as the time-averaged gradient, so the gradient blips are not taken into account:

$$G_{acq} = \frac{N_{pe}}{\gamma L_{pe} T_{acq}} \tag{2}$$

Where N_{pe} and L_{pe} are the number of voxels and FOV in the phase-encoding direction, respectively, and T_{acq} is the acquisition time. T_{acq} is usually minimized, based on hardware constraints. This means that G_{acq} can only be increased further by decreasing Δy_{pe}, which is often not possible without decreasing the FOV in phase-encoding direction, which could lead to fold-in artifacts.

Signal dropout can occur due to increased T_2'-dephasing, as a result of increased spin-spin interactions when there are large variations in the local magnetic field e.g. at air-water interfaces. Dephasing due to static field inhomogeneities can be compensated by spin-echo approaches to a certain degree; only the center of k-space is completely refocused and dephasing due to temporally changing interactions, i.e. diffusion effects, can never be refocused.

All of these artifacts; distortion, chemical shift and signal dropout are addressed in spatio-temporal encoding (SPEN). In SPEN G_{acq} does not depend on Δy_{pe}, as in EPI[63]. Thereby, the use of a larger G_{acq} is enabled, reducing distortion and chemical shift artefacts. In addition,

SPEN can be employed in the full-refocusing mode where every data point is refocused instead of just the center of k-space, reducing signal drop out[63].

In SPEN, excitation is performed using a combination of a frequency swept chirp pulse with a gradient, see Figure 1a. The linear dependency of frequency on space leads to a quadratic phase profile[180]. The quadratic phase profile results in excitation of the spins which are located at the vertex of the quadratic phase profile, while the spins located further away from the vertex undergo rapid dephasing. This point of excitation will move over the FOV linearly in time due to G_{exc}, resulting in a sequential excitation of voxels in time. Spins acquire a phase build-up during excitation by G_{exc}, depending on spatial location. This phase build-up is unwounded sequentially by blips of G_{acq} during acquisition to create an echo, according to[64]:

$$G_{exc}T_{exc} = G_{acq}T_{acq} \tag{3}$$

Where G_{exc} and T_{exc} are the gradient strength and duration of the frequency-swept CHIRP pulse, respectively, and T_{acq} is the acquisition time. G_{exc} is defined as:

$$G_{exc} = \frac{BW_{exc}}{\gamma L_{pe}} = \frac{Q}{\gamma L_{pe}T_{exc}} \tag{4}$$

Where L_{pe} is the FOV in phase-encoding direction and Q is defined as:

$$Q = BW_{exc}T_{exc} \tag{5}$$

Using equation 3 and 4:

$$G_{acq} = \frac{Q}{\gamma L_{pe}T_{acq}} \tag{6}$$

So when scanning SPEN, Q needs to be > N_{pe}, to benefit from less distortions compared to EPI, see equation 2. Another benefit of using SPEN is that if T_{exc} is chosen such that:

$$T_{exc} = T_{acq} \tag{7}$$

and the 180-degree refocusing pulse is placed symmetrically between G_{exc} and G_{pe}: all spin packages will refocus exactly at the time of their readout. This results in full T_2'-refocusing in phase-encoding direction, preventing signal loss due to dephasing[63]. Furthermore, T_{exc} and thus T_{acq} should be kept to a minimum for a given Q, to prevent signal loss due to T_2-decay. This provides a challenge for ASL body applications, where the desired FOV is usually relatively large.

The variable Q will determine the sweep rate R of the chirp pulse, see equation 6, and the sweep rate R will in turn determine the spatial width Δy_{exc} of the excitation for each measurement point[64].

$$R = \frac{BW_{exc}}{T_{exc}} = \frac{Q}{(T_{exc})^2} \tag{8}$$

$$\Delta y_{exc} = \frac{\sqrt{R}}{\gamma G_{exc}} \tag{9}$$

It is important to note here that Δy_{exc} does not determine the voxel size Δy_{pe}. The width of excitation Δy_{exc} will determine the locality of spins that are excited for the measurement of one voxel, and thereby the encoded resolution and SNR[64]. A wider excitation will generate more signal, but will also create blurring as more signal of neighboring spins will be excited. With the use of super-resolution reconstruction[64] the acquired signal can be de-convolved, using the simulated excitation profile, to remove this blurring. When using super-resolution reconstruction it is beneficial to use a larger Δy_{exc}, so that multiple excitations can be averaged for one voxel, increasing SNR and allowing similar SNR-levels as EPI[156], [162]. So to increase SNR, R, and thus Q, should be minimized, since T_{exc} ($=T_{acq}$) is constrained by hardware. This poses a trade-off with robustness to field inhomogeneity, which requires a higher Q to increase G_{pe}. The optimal Q is the minimum value that provides robustness to the envisioned ΔB_0, and thus is dependent on the application.

Because the FOV is not excited at one instant in time the relationship between required B_1 for a certain flip angle θ is more complex, and is determined by simulations. For a $\theta = \frac{\pi}{2}$ this results in[163]:

$$B_1 = 0.27 * \frac{\sqrt{R}}{\gamma} \tag{10}$$